IEEE Access
Multidisciplinary ⋮ Rapid Review ⋮ Open Access Journal

Received 24 October 2023, accepted 26 November 2023, date of publication 4 December 2023,
date of current version 28 December 2023.

Digital Object Identifier 10.1109/ACCESS.2023.3339196

RESEARCH ARTICLE

Task Allocation for Multi-Agent Specialized Systems Using Probabilistic Estimate of Robots Competencies

OMAR AL-BURAIKI[1,2], (Member, IEEE), AND PIERRE PAYEUR[1], (Member, IEEE)
[1]School of Electrical Engineering and Computer Science, University of Ottawa, Ottawa, ON K1N 6N5, Canada
[2]Department of Mechanical and Mechatronics Engineering, University of Waterloo, Waterloo, ON N2L 3G1, Canada

Corresponding author: Omar Al-Buraiki (omar.alburaiki@uwaterloo.ca)

This work was supported by the Innovation for Defence Excellence and Security (IDEaS) Program through the Government of Canada.

ABSTRACT An innovative task allocation scheme for a multi-robotic system in a specific context is introduced in this paper, where functionalities of the individual robots are considered, and a probabilistic estimate of each robot specialization is computed. The problem is formulated based on the assumption that each robotic agent is qualified for performing specialized functionalities, and the expected tasks distributed in the surrounding environment enforce specific requirements. The task allocation algorithm evolves through three stages to compute individual robot allocation probabilities. First, recognizing the features of the target task is addressed by leveraging the output of a vision system in the sensing layer to drive the proposed agent-task allocation scheme. Second, a matching strategy is formulated to match each robot's unique functionalities with the corresponding features of target tasks. The specialization of each agent is developed in two approaches as a main part of the matching process: first, a binary association of the capabilities of each agent, and second, based on the suitability of each agent to tackle the various tasks. Finally, the developed robot-task-matching system is expanded to fully utilize the potential of the robot specializations, considering the agents attendance level with the availability of services of each agent. The developed framework is extensively validated through MATLAB simulations. To demonstrate the feasibility of the proposed system for real-life applications, the developed framework is implemented on real robots. The results show that the performance of the proposed allocation scheme is increased significantly when the suitability levels of the agents' specializations inform the task allocation process and agent attendance levels are activated.

INDEX TERMS Robot-task matching, heterogeneous robotic system, robots' specialized functionalities, probabilistic estimation of specialization.

I. INTRODUCTION

Recent advances in autonomous robotic systems are promising to shape future industries and services such as public spaces surveillance operations [1], search and rescue applications [2], sample and data collection in large manufacturing plants and dangerous places [3], maintenance operations [4], logistic services [5], emergency first responders [6], and military operations [7]. This research aims to evolve the multi-robot team to function as a cooperative team of specialized robotic agents based on formal consideration of each individual robot's specialization. As a result, the individual robots should be able to reliably perform a diversity of tasks while focusing on specialization. This leads to efficient distribution of the workload, where each task is to be fully or partially primary by an individual or multiple agents among the robotic team. This paper focuses on the formulation of the individual robots' specialization. Solutions are proposed for a multi-agent system of specialized robots to be efficiently assigned to allocate target tasks that impose specific requirements for their successful completion, a perspective that has not yet been extensively addressed in the literature. This paper is a substantially extended and reformulated version of [8] in terms of both implementation details and experimental

The associate editor coordinating the review of this manuscript and approving it for publication was Dominik Strzalka.

TABLE 1. Comparison of the proposed approach to three state-of-the-art task allocation methods.

Task Allocation Approach	Utility function	Constraints		Location		Control Strategy		Applications
		Task	Agent	Agent's location	Target's location	Centralized	De-Centralized	
Specialty-Based Approach (proposed)	- Target-agent matching probability - Target-agent distance - Agents' availability - Agents' attendance	Target features (task requirements)	Agent's specialized capabilities	√	√	Hybrid √ Centralized in Task-Space.	√ Decentralized in Control-Space	- Firefighting - Search-and-rescue - Service robotics - Military/security - Parcel delivery - Public transportation
IDTA [29]	- Agents' waiting times at task interface	Target location	Agents' arrival times	×	√	×	√	- Service robotics
MTSA [30]	- The distance between the agent and the task	Minimal length of the travelled trajectory		√	√	×	√	- Exploration tasks
SOCM [31]	- Euclidean distance	Target features	Agent's resources	√	√	√	×	- Search-and-rescue
MOACS [42]	- Balancing cost of the robotic agent and the workload.	×	- Flight speed. - Execution Time.	×	√	√	×	- UAV in general as an optimization approach.
HGSA [43]	- Agents' waiting times at task interface	Target location	- Number of the recourses	√	√	√	×	- Military/Security

validation. The contribution of this paper focuses on designing a task allocation framework for a diverse group of robotic agents based on their specializations, where the agents' specific mechanical or instrumental traits are represented in two ways: either a binary specialization definition, or a refined version indicating their suitability for various tasks, which outperforms the binary specialization by multiple times as indicated by experimental results on test cases. The proposed approach links the agents' specialized functions to visually detected features of target objects with confidence level. This information is utilized in a novel task-agent probabilistic matching scheme that calculates agents' specialty-based task allocation probability. Then, the framework is extended to automatically assign qualified agents to the corresponding tasks considering their availability state and attendance level. The results indicate that the extended framework outperforms the original one and presents an effective coordination and adaptability on workspaces of varying sizes and complexity.

The following section reviews the related approaches for automated task-agent allocation. Section III outlines the presented framework in detail, while section IV addresses the recognition process of the task characteristics that defines the target object considered. The design aspects of the task-agent speciality matching scheme as well as the qualified responders' coordination are introduced in Sections V and VI respectively which represents the main contribution of this paper. Section VII discusses the observations on simulation experiments. Finally, the proposed framework is implemented on real robots and the results are reported in Section VIII.

II. RELATED STUDIES

Previous art in the field of task-agent allocation introduced many solutions for the coordination of multi-robot systems [9], [10]. An optimal sequence of task allocation that minimizes the time of the assignment process or reduces the cost of energy consumption for a multi-robot system of heterogeneous agents is developed in [11]. The stick-pulling approach [12] is used in [13] to study the advantages of specialization when two robotic agents are required to accomplish a joint task. This work is extended in [14] for any number of robots, based on individual adjustments to the agents. The robots are initialized to search for randomly distributed sticks in their vicinity. A task-partitioning strategy to split the task of object retrieval between the source and a nest into sub-tasks is introduced in [15] and [16]. A behavioural specialization [17] in a multi-agent robotic team is introduced as a result of interactions among the robotic agents and their environment. Two constrained resources are considered in [18], where a first set of robots can only feed from one specific resource while another set feeds from the other resource. Alternatively, an auction algorithm is proposed in [19] that enables every robot to independently define a task to be assigned to. The above-mentioned studies address the task-robot assignment cost as a function of the distance that the robot needs to travel to the target task, the time, or the power that is required to accomplish a defined task. However, these studies do not leverage the characteristics of the robotic agents' specialized capabilities.

Alternatively, a task-robot task allocation probabilistic approach is introduced in [20] to divide the environment containing targets into a network of cells. Then, the robots that are available in each cell are assigned to the targets that occupy the same cell. Another probabilistic framework that defines object-action relevance is addressed in [21], but the features of the objects are not estimated for a convenient matching process. This model is utilized in [22] to compute a series of behaviours and apply estimated inference to manage the robot's planning, grasping, and reasoning for the arrangement of table-top items. In a different context, a probabilistic threshold-based control approach is introduced in [23] to derive the robots to perform a food-foraging process. However, the individuals can only perform two tasks of nesting and searching, thereby limiting the scope of specialization application.

Recently, many works have addressed the task allocation of multi-robot systems [24].The recent developments in the field focus on combining the generalized formulations of the task allocation problem and recent advances in swarm intelligence [25], or on the task planning aspects, such as task scheduling as a simultaneous process of task allocation, rather than introducing a formal specialization definition based on the individual agents' functionalities within a heterogeneous robotic team. A game-theory-based coalition framework is also addressed in [26] to coordinate and form robotic teams with different sensing capabilities to collaborate and accomplish tasks. The proposed approach does not address the formal specializations of the individual robots as standardized probabilistic scores based on the individual robots' functionalities (sensors, actuators, software, fuel, battery, availability, attendance). As well, the proposed approach in [26] does not address the assignments of the most qualified or all qualified robots based on the application's demand but rather on the framework's flexibility to accommodate medium, and wide task spaces.

Based on existing literature, a significant technological gap among potential solutions is identified, which is the consideration of a formal specialization definition based on the individual agents' functionalities among a group of robots. Table 1 outlines the primary distinctions between the proposed approach and existing literature in the domain of multi-agent robotic teams.

To maximize the benefits of teamwork within a heterogeneous robotic team composed of agents that possess such specialized capabilities, a probabilistic mechanism for task-agent matching is proposed in this paper to encode and utilize the robots' specialization and achieve competent strategic task assignment of the individual robots to allocate target tasks. This paper puts forward noteworthy contributions extending beyond the authors' previous publications [27], [28], as the original task allocation process is extended and developed in three stages. First, a task features recognition stage was conceptually introduced to utilize the output of a sensing layer embedded in robotic agents for driving the proposed task allocation scheme. This stage is discussed in Section IV. Second, a matching scheme was developed to best match each agent's specialized capabilities with the corresponding detected tasks. At this stage, a general binary definition of agents' specialization is defined to serve as the foundation for task-agent association. Then, the framework is generalized and further refined with a modulated definition of the agents' specialization based on their mechanical and physical structure, as well as embedded resources. This stage is addressed in Section V. Finally, the developed task-agent matching scheme is expanded to fully utilize the potential of individual robotic agents' attendance level and their availability in services to coordinate the qualified agents for allocating the detected tasks. This coordination stage is presented in Section VI. This paper studies closely the impact of diverse specialization management strategies in operational conditions through an extensive experimental validation.

III. PROPOSED FRAMEWORK

The developed framework builds upon a probabilistic task allocation process for a team of heterogeneous robots to match them to constrained tasks. The individuals of this team are equipped with specialized functionalities. The tasks are distributed in the surrounding environment, and their detection imposes specific allocation requirements. The solution considers the individuals of the robotic team to have various levels of functionality (i.e., physical construction, sensors, actuators, communication and cognitive capabilities, or operational capacities). This constructs a robotic system offering varying suitability levels of robot-task allocation responses in terms of the robots specialized capabilities and the task allocation requirements. To achieve this objective, two spaces are developed to ensure suitable coordination between the specialized robots and the corresponding tasks. A schematic diagram of the proposed system is shown in Fig. 1. The control space carries out the control sequences to drive the robots to the positions of the detected task, such as dynamic stabilization, navigation, team formation, and path tracking control. The design aspects of the control space are addressed by the authors in a prior work [32]. On the other hand, the specialization space addresses the problem of matching the detected task's requirements with the specialized capabilities of the available members of the robotic team. This represents the main contribution of this article.

A robot-task probabilistic matching approach is developed in the specialization space to match distinctive features identified on detected tasks with the robots' embedded specialized resources. The approach depends on an uncertain representation of detected features on target objects (task features) [33], which defines a specific signature of the detected task to be matched with the functionalities of the individual robots. This paper addresses the framework design from three main perspectives: 1) recognition of the target task; 2) robot-task probabilistic matching; and 3) suitable responders' coordination. The developed automatic task selection unit (ATSU), as illustrated in Fig. 1, is responsible for the decision-making process [36]. ATSU ensures the allocation of the most qualified robot, or robots, to a corresponding detected task. The latter takes the form of a target detected with a vision sensor.

IV. RECOGNITION OF TASK CHARACTERISTICS

To guide the task allocation process, observable features perceived on target objects with robot-embedded vision sensors are considered in defining the nature of a given task to be fulfilled by agents belonging to the robotic system. The characteristics of the expected target objects are split up into classes. Each class of target objects is encoded as a vector of N sample features, that is $\boldsymbol{X}_k = \{x_j : j = 1, 2, 3, \cdots, \mathcal{N}$, given that $x_j \in \mathcal{R}^{\mathbf{2}}$ is a two-dimensional spatial feature. For the sake of generality, in this formulation, the assumption made was that x_j is a Gaussian distributed random sample of a spatial feature observed in 2D with mean μ and covariance σ^2. It is also assumed that $k = 1, 2, 3, \ldots, T$, where T is the determined number of the target's classes that may be detected

over a defined tasks space, $\boldsymbol{X} = [\boldsymbol{X_k}{:}k = 1, 2, 3, \ldots, T]$, and each group of features $\boldsymbol{X}_k$ is related to one specific class, $C_l{:}l = 1, 2, 3, \ldots, T$. Samples from these classes are considered available for training a deep learning-based target detection stage. To map the suitable robotic agent/agents to the equivalent target-task independently, each class C_k of the target objects is linked with an action of a specific response to be performed by the embedded specialized functionality of a robotic agent. Therefore, a well-defined task space $\boldsymbol{X}$ consists of $\mathcal{N}\times T$ features to be performed by the available specialized/heterogeneous functionalities of the robotic team. A pre-trained deep learning network with a corresponding set of T classes is used to retrieve any observed $\boldsymbol{X}_k$ based on the visual observation of the target object [34]. The perception system is generalized in this formulation. The target object detection is computed by the Bayesian posterior probability:

$$P\left(C_l \mid \boldsymbol{X}_k\right) = \frac{p(\boldsymbol{X_k}|C_l)P(C_l)}{p(\boldsymbol{X_k})} \tag{1}$$

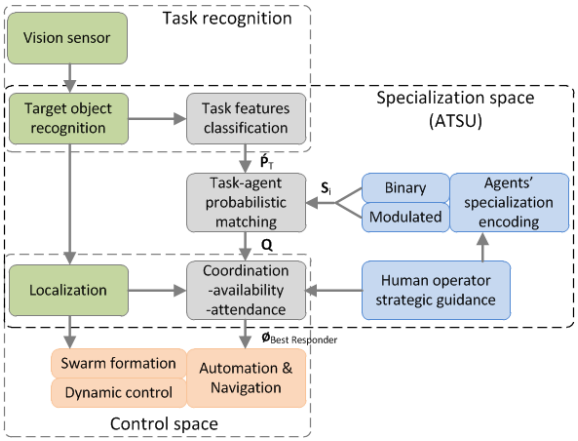

FIGURE 1. The architecture of the proposed framework for specialization-based robot-task allocation and control.

where the Gaussian distribution of the feature $\boldsymbol{X}_k$ in each class C_l is described by a class-conditioned probability density function $p(\boldsymbol{X}_k|C_l)$. $P\left(C_l\right)$ is the prior probability of the class C_l in the given training dataset, and $p(\boldsymbol{X}_k)$ is given by:

$$p\left(\boldsymbol{X}_k\right) = \sum_{l=1}^{T} p(\boldsymbol{X}_k|C_l)P(C_l) \tag{2}$$

given that all quantities of $P\left(C_l \mid \boldsymbol{X}_k\right)$, defined in Eq. (1), are functions of the classes C_l except $p(\boldsymbol{X}_k)$. As such, the denominator in Eq. (1) can be considered a normalization constant. Therefore, it can be substituted by $\frac{1}{\xi}$ to integrate the left-hand side to one. Thus, the posterior probability is evaluated as:

$$P\left(C_l \mid \boldsymbol{X_k}\right) = \xi p\left(\boldsymbol{X}_k \mid C_l\right) P\left(C_l\right) \tag{3}$$

In practice, a deep learning network [20] is trained from the sample image dataset of the classes C_l's of features $\boldsymbol{X}_k$'s representing various objects to perform target task-object detection. The latter then provides an input to the proposed task allocation framework as shown at the top of Fig. 1.

V. TASK-AGENT SPECIALTY MATCHING SCHEME

General concept: For a given match, a robot should respond to a given task only when it offers a sufficient specialty-based competencies probability in the presence of the detected task requirements. The latter are inferred from the detected features of the target task while robot competencies are pre-defined by its physical characteristics. In addition, a given robotic agent can also be qualified for different tasks but with different levels of specialty-fitting probabilities. The proposed task-robot matching scheme runs two functions: 1) to calculate the robot-task specialty-fitting level between the robotic agents and the detected task; and 2) to dynamically allocate the detected task to the most specialized and available agent or agents.

A. INDIVIDUAL ROBOTS' SPECIALIZATION ENCODING

A heterogeneous robotic team $\{R_i, i = 1, 2, 3, \ldots\ldots, M\}$ encompasses M specialized robotic agents and supports T different specialized roles or functionalities corresponding to the number of target object classes that can be detected. In this research, two different representations are considered to encode specialized functionalities:

1) BINARY ENCODED TASK ALLOCATION (BETA)

The specialized roles or functionalities of each robot are defined in a binary vector: $\boldsymbol{S}_i{:}\{\mathrm{s}_k, k = 1, 2, \ldots, T\}$ where $\boldsymbol{S}_i \in \mathcal{R}^{1\times T}$. Every entry in $\boldsymbol{S}_i$ is defined as:

$$\mathrm{s}_k = \begin{cases} 1 & : R_i \text{ possesses a corresponding functionality.} \\ 0 & : R_i \text{ does not possess a corresponding functionality.} \end{cases} \tag{4}$$

$\mathrm{s}_k = 1$ indicates that the robot, R_i, holds the corresponding functionality to tackle a task of a given class C_l; and $\mathrm{s}_k = 0$ means that the robot, R_i, is not provided with the necessary attribute required to perform a task of a class C_l. For example, consider a firefighting scenario in which individual agents within a heterogeneous robotic team are equipped with diverse capabilities for combating fires in various settings, including large residential complexes, skyscrapers, small houses, and warehouses. The primary task classes are residential complexes, skyscrapers, small houses, and warehouses. In this case, the specialization vector of each agent R_i is defined as $\boldsymbol{S}_i{:}\{\mathrm{s}_k, k = 1:4\}$. The binary encoding of the agents' heterogeneous specializations is suitable for assigning a qualified robot to a detected task, provided that the robotic agent possesses a corresponding capability in relation to the detected class associated with the target object, regardless of the suitability level of the processed capability concerning the detected target class. In the following section, the definition of agents' specialization is modeled in a non-binary form, not only for assessing their capability possession

but also to account for varying levels of sophistication in their specialized capabilities. This differentiation is rooted in the agents' mechanical construction, embedded hardware, and software, with the aim of capturing different levels of suitability of the agents' specialization for different tasks.

2) MODULATED ENCODED TASK ALLOCATION (META)

To provide additional flexibility in the task allocation process, the binary definition of the agents' specialty vector, $\boldsymbol{S}_i$, introduced above, can alternatively be modulated in a non-binary form. This modulated representation of the agents' specialization is adopted when increased sophistication of the task allocation scheme is either necessary or permitted by the application. Human beings may be considered as an example, given that individuals have many talents, but some are more developed than others, and some are physically stronger or in better shape than others. For example, if a group of people enter a marathon, all of them may be able to complete the marathon successfully. However, they would not finish at the same time due to differences in training and physical condition. This example highlights that the purpose of modulating specialized capabilities is to emulate the natural diversity and robustness of individual agents' skills at varying levels of functional competence concerning specific objectives. Therefore, reformulating specialization as a modulated encoding is a more accurate representation of individual agents' potential, whereas a binary-only specialty vector falls short in capturing the full range of their specialized capabilities. Let's assume that the entries of $\boldsymbol{S}_i \in \mathcal{R}^{1\times T}$ are modulated to take values over the continuous range from 0 to 1, such that $s_k \in [0\ 1]$, to represent the relative level of the agents' specialized suitability from the least efficient (0) to the most efficient (1), to tackle a task of a class C_l recognized from the observed group of features, $\boldsymbol{X}_k$. The specialization encoding is then revisited as:

$$s_k = \begin{cases} 0 < s_k \leq 1 & : R_i \text{ possesses a level of corresponding functionality.} \\ 0 & : R_i \text{ does not possess a corresponding functionality.} \end{cases} \tag{5}$$

B. PROBABILISTIC ESTIMATE FOR TASK-AGENT MATCH

The agent-task specialty fitting probability is determined for an individual robotic agent of identity, i, in accordance with the constraints raised by the detected classes on target objects as per the discussion in Section IV. To compute each robot speciality estimate, each robot offers a unique specialty fitting level, $\hat{\varphi}_{R_i}$, considering its specialized capabilities, $\boldsymbol{S}_i$,. This level is estimated as:

$$\hat{\varphi}_{R_i} = \boldsymbol{S}_i \hat{P}_T \tag{6}$$

where $\hat{\varphi}_{R_i} \in \mathcal{R}^{1\times 1}$ is scalar. $\hat{P}_T \in \mathcal{R}^{T\times 1}$ represents the probability transition vector of the detected classes on target objects, that is an uncertain classification from the target object recognition stage. This is formulated as a vector of estimated posterior probabilities, Equation (3), which is expressed as follows:

$$\hat{P}_T = \left[\sum_{k=1}^{T} P(C_1 \mid \boldsymbol{X}_k) \sum_{k=1}^{T} P(C_2 \mid \boldsymbol{X}_k) \ \cdots \ \sum_{k=1}^{T} P(C_T \mid \boldsymbol{X}_k) \right]^T \tag{7}$$

To express the task-agent specialty matching in a probabilistic form, the concepts of probability theory are adopted [35]. In this formulation, the specialized capabilities (i.e., the heterogeneous equipment that each robot possesses, such as sensors, actuators, computation resources, and communication links) are encoded in its specialization vector, $\boldsymbol{S_i}$. The overall outcome is estimated as an agent's specialty fitting level, $\hat{\varphi}_{R_i}$, defined in Eq. (6), which is a function of the agent's specialization vector, $\boldsymbol{S}_i$, and uncertain recognition of target objects, $\hat{P}_T$. Finally, a corresponding specialty fitting probabilistic score, Q_i, over the range [01] is defined for each individual robotic agent as their respective fitting probability for a detected task or target. This probability is computed by normalizing each agent specialty fitting level, $\hat{\varphi}_{R_i}$, by its specialty collective score, φ_{R_i}, that is computed when all of the robot's capabilities/specialized roles (Eqs. 4 and 5) are in fit with all potential target classes C_l:$l = 1, 2, 3, \ldots, T$. φ_{R_i} is defined in Eq. (9). Therefore, the specialty fitting probability of each robot, R_i, can be calculated as follows:

$$Q_i = \frac{\hat{\varphi}_{R_i}}{\varphi_{R_i}} \tag{8}$$

The maximum collective score, φ_{R_i}, of a robot R_i is defined as:

$$\varphi_{R_i} = \boldsymbol{S_i} \boldsymbol{p}_{max} \tag{9}$$

and;

$$\boldsymbol{p}_{max} = [p(\boldsymbol{X}_1|C_1)\, p(\boldsymbol{X}_2|C_2) \ \cdots \ p(\boldsymbol{X}_T \mid C_T)]^T \tag{10}$$

where $p(\boldsymbol{X}_k \mid C_l)$ is the class-conditional probability of $\boldsymbol{X}_k$ in its predefined class. For more detailed information on computing class-conditioned probabilities, interested readers can refer to [35]. In practice, it is reasonable to consider $\varphi_{R_i} = \sum_{k=1}^{T} s_k$, which is the sum of the encoded agent's specialized roles/capabilities as per Eqs (4 and 5). As a result, a diagonal swarm's probabilistic matching matrix $\boldsymbol{Q} \in \mathcal{R}^{M\times \mathrm{M}}$ is introduced, which formally accommodates the probabilistic estimate of each robot's specialization to respond to specific task/target, defined as:

$$\boldsymbol{Q} = diag[\frac{\hat{\varphi}_{R_1}}{\varphi_{R_1}}, \frac{\hat{\varphi}_{R_2}}{\varphi_{R_2}}, \ldots, \frac{\hat{\varphi}_{R_{M-1}}}{\varphi_{R_{M-1}}}, \frac{\hat{\varphi}_{R_M}}{\varphi_{R_M}}] \tag{11}$$

VI. QUALIFIED RESPONDERS' COORDINATION

Beyond reliably associating robotic agents to allocate detected targets in the environment, it is also important to support realistic scenarios in which an agent may not always be available because of faulty conditions that prohibit the robot from performing its duties. Alternatively, a robot may be already involved in another task or be located far from the

target position when called to service by the task allocator. To tackle such situations, the proposed framework is refined to formally consider the agents' availability state ϑ_{Av}, and attendance level ϑ_{Att} along with their specialty fitting probability $\boldsymbol{Q}$.

A. AGENTS' AVAILABILITY AND ATTENDANCE

The robotic agents' availability, ϑ_{Av}, is an original attribute of this framework that improves its reliability to achieve the mission goals by replacing the allocations of qualified but unavailable robotic agents with alternative available and partially qualified robots.

The availability vector $\vartheta_{Av} \in \mathcal{R}^{M\times 1}$ is defined based on the status of the robot's being in service. At the moment of robotic team deployment, an internal flag of the deployed robots is turned to "available" to declare the viability state of each given robot, while the same flag for robotic agents that are not in service is turned to "withdrawn" to declare the unavailability state. The robotic agents that are in the "withdrawn" state cannot be assigned for the task allocation. However, the system automatically searches for an alternative "available" robotic agent with an appropriate specialty fitting probability to fulfil the task allocation goal. In addition, when an available agent is assigned to a given task, its availability state is changed to "busy," which indicates to the task allocator that the agent is temporarily unavailable. The availability status vector of the swarm members, $\vartheta_{Av} \in \mathcal{R}^{M\times 1}$, is defined as:

$$\vartheta_{Av_i} = \begin{cases} 1, & R_i \text{ is "}available\text{"} \\ 0, & R_i \text{ is "}withdrawn\text{" or "}busy\text{"} \end{cases} \tag{12}$$

In addition, a diagonal attendance matrix, $\vartheta_{Att} \in \mathcal{R}^{M\times \mathrm{M}}$, is defined based on the distance, d_i, between the current position of every robot and the position of the detected target. The distance, d_i, is taken into consideration with the objective to optimize the time response of the qualified individuals among the swarm by privileging closer agents to address tasks in their neighbourhood. Beyond the respective displacement, the concept of attendance also considers the relative velocity of the individual robotic agents, v_i, and the velocity of the detected target , v_t. This proves essential when dealing with moving target objects to ensure that the available agents are sufficiently fast to reach the assigned targets. The respective robots' attendance levels are evaluated at the moment a target object is detected. The role of the corresponding weights defined as in Eq. (14), shown at the bottom of the page, is to influence the robots' specialty fitting level and to increase the probability of assigning the closer agents. The attendance matrix of the swarm is formed as:

$$\vartheta_{Att} = \begin{bmatrix} \vartheta_{Att_1} & 0 & \cdots & \cdots & 0 \\ 0 & \vartheta_{Att_2} & & & \vdots \\ \vdots & & \ddots & & \vdots \\ \vdots & & & \ddots & \vdots \\ \vdots & & & \vartheta_{Att_{M-1}} & 0 \\ 0 & \cdots & \cdots & 0 & \vartheta_{Att_M} \end{bmatrix} \tag{13}$$

with, where d_i is the route length (Euclidean distance) between the current location (x_i, y_i) of the robot R_i and the location of the detected target object (x_T, y_T) in their shared 2D plane. r_{task} is the radius of the designated task zone [36] of influence which represents the maximum spread of candidate target objects around a given robotic agent, and it is tuned by the system's designer. v_i is the current linear velocity of the robot R_i. $v_{i_{max}}$ is the maximum pre-initialized limit of the linear velocity of a robot R_i. v_t is the linear velocity of the detected target, defined positive when the target moves in the same direction as the agent's movement and negative when the agent and target move in opposite directions. $\bar{\mathrm{T}}$, ϵ, and Υ are control variables that take binary values, 1 or 0, to turn on or off the effect of the robots' velocity and the distance to the target location based on sensors outputs that estimate relative distance and velocity of the robot and target objects. The binary value of $\bar{\mathrm{T}}$ is defined based on the comparison between the estimated velocity of the target and the maximum predefined velocity for each agent. When $v_t \geq v_{i_{max}}$, then $\bar{\mathrm{T}}$ equals 0 and the weight of the agent's attendance term in Eq. (13) is null. As a result, the target cannot be reached as long as its velocity is higher than or equal to the agent's maximum velocity. The task allocator then automatically disengages the corresponding agent. For the sake of validation, the discussion in this paper is limited to cases of static targets (i.e., $\epsilon = 0$).

B. COORDINATION SCHEME

The overall proposed task-agent coordination scheme is synthesized as a summation of two components: fixed specialty fitting probabilities, $\boldsymbol{Q}$, weighted by a ratio, ρ, and a varied

$$\vartheta_{Att_i} = \begin{cases} \dfrac{\bar{\mathrm{T}}\left(\epsilon\left(\frac{v_i}{v_{i_{max}}}\right)+\left(\frac{r_{task}}{d_i}\right)^{\Upsilon}\right)}{2^{\epsilon}} & \begin{cases} \Upsilon = 1\{d_i > r_{task} \\ \Upsilon = 0\{d_i \leq r_{task} \\ \epsilon = 1\{moving\ target \text{ AND } v_t \text{ is positive} \\ \epsilon = 0\{static\ target \text{ OR } v_t \text{ is negative} \\ \bar{\mathrm{T}} = 1\{v_t < v_{i_{max}} \\ \bar{\mathrm{T}} = 0\{v_t \geq v_{i_{max}} \end{cases} \\ 0, & \{R_i \text{ is "}withdrawn\text{" or "}busy\text{"} \end{cases} \tag{14}$$

agents' attendance level, $\boldsymbol{\vartheta}_{Att}$, weighted by $(1-\rho)$. These two components are further filtered by the agents' availability status, $\boldsymbol{\vartheta}_{Av}$.The overall task allocation scheme is defined as:

$$\boldsymbol{\Psi} = (\rho \boldsymbol{Q} + (1-\rho)\boldsymbol{\vartheta}_{Att})\, \boldsymbol{\vartheta}_{Av} \tag{15}$$

$\boldsymbol{\Psi} \in \mathcal{R}^{M\times 1}$ returns the task allocation probabilistic fitting levels for every available agent, or 0 for withdrawn or busy robots, with respect to the latest detected task. The parameter $\rho \in [01]$ is defined by the system's designer to distribute the weight of the overall task allocation fitting probabilities between $\boldsymbol{Q}$ and $\boldsymbol{\vartheta}_{Att}$ based on the nature of the application. For example, in applications where specialty matching between the agents' functionalities and corresponding targets is predominant over the time it takes for the swarm to respond, such as in service robotics, then ρ can be set close to its maximum (1). However, in applications such as emergency response, where the agents' attendance (proximity and velocity to shorten response time) is predominant, then ρ can be set to lower values, according to the amount of specialization that is still expected. As a result, a balance between specialization and time efficiency can be achieved.

C. HUMAN STRATEGIC GUIDANCE

To provide the system with strategic guidance, a role is given to a human supervisor in the control loop to influence the behaviour of automated process when needed [37], [38], [39]. The framework preserves such an access on the operational loop to initialize or to modify the system's operational conditions and provide a form of strategic guidance to the task allocation process, as shown on the right side of Fig. 1. For this purpose, a minimum fitting threshold (MFT) η is applied as a protection measure that ensures a minimum matching probability below which no robot can be assigned. The main role of the human supervisor is designed to dynamically control the MFT level. The human supervisor can have access to adjust this parameter either before the deployment of the robotic team or during operation. The MFT can be selected at different levels between 0 and 1 based on the operating conditions of the application or in association with the application's requirements. This way, human awareness of the situation can be combined with the automated process by modifying this parameter, and a level of trust in the task allocation process can be influenced.

A desired objective of the proposed solution is to reduce the cognitive load on the human supervisor. Pre-setting the distribution of MFT over two ranges can reduce the number of times the human operator needs to intervene on the MFT set point. Therefore, the desired MFT, η, is defined as $\eta \in (01]$ but is distributed over two predefined ranges forming a low specialty fitting level (LSFL) and a high fitting level (HSFL). The lower range, LSFL, is defined with $\eta \in (0B]$ to drive the task allocation process to meet the minimum specialized functionalities of the available robots to allocate to the detected tasks. On the other hand, in situations where a higher level of trust in the task allocation process must be ensured to match only the most capable robotic agents with the requirements of the detected tasks, the human supervisor easily switches the process to work in HSFL range, $\eta \in (B1]$. For applications that involve a level of attendance, $\boldsymbol{\vartheta}_{Att}$, in Eq. (15), to boost the specialty fitting probability, $\boldsymbol{Q}$, the low specialty fitting level (LSFL) is conditioned to $(1-\rho) < \eta$ which leads to:

$$\begin{cases} LSFL: & (1-\rho) < \eta \leq \mathrm{B}, \\ HSFL: & \mathrm{B} < \eta \leq 1, \end{cases} \tag{16}$$

This formulation ensures that the level of the agents' attendance, $\boldsymbol{\vartheta}_{Att}$, would only boost the specialty-based matching probability, $\boldsymbol{Q}$, but $\boldsymbol{\vartheta}_{Att}$ cannot initiate the task allocation process without a required level of the agents' specialty. Therefore, $\boldsymbol{\Psi}$, defined in Eq. (15), is further refined to only consider the task allocation fitting probabilities of the available agents that achieve the desired MFT, which is redefined as $\boldsymbol{\Psi}_{MFT} \in \mathcal{R}^{M\times 1}$:

$$\boldsymbol{\Psi}_{MFT} = [\Psi_{MFT_1}, \Psi_{MFT_2}, \cdots, \Psi_{MFT_M}]^T \tag{17}$$

where,

$$\Psi_{MFT_i} = \begin{cases} \Psi_i, & |\Psi_i \geq \eta : \Psi_i \in \boldsymbol{\Psi} \\ 0, & |\Psi_i < \eta : \Psi_i \in \boldsymbol{\Psi} \end{cases} \tag{18}$$

Accordingly, the qualified available agents are automatically selected and allocated to the detected tasks considering the human supervisor's strategic guidance. The identification index of the best-suited available agent above the MFT is given by:

$$\emptyset_{BEST\ RESPONDER\ INDEX} = i | i \in max\{\boldsymbol{\Psi}_{MFT}\} \tag{19}$$

The use of the *max* operator is to extract either the identification index of a single agent with the highest fitting probability, or alternatively a group of identification indexes if multiple agents share the same fitting probability. In the latter case, when more than one agent shares the highest score, the *max* operator extracts their identification indexes sequentially based on their order in the vector of Eq. (17). Alternatively, when the goal is to allocate all of the qualified agents to the detected task, an iterative loop runs inside the vector of Eq. (17) to extract identification indexes of all the agents that achieve the desired MFT.

VII. EXPERIMENTAL STUDY

Experiments are conducted to validate and evaluate the efficiency of the proposed approach in simulations and on physical robotic platforms (Section VIII). First, the proposed system is tested in simulation trials and exemplified by $T = 14$ classes of target objects that can be potentially detected in an environment where a swarm consisting of $M = 20$ specialized robotic agents operate. Tables 14 in appendix provides a binary representation of competencies (BETA) for each of the 20 agents considered based on the agents' embedded specialized functionalities, as defined in section V-A.1. Conversely, Table 15 in appendix provides a modulated representation of competencies (META) for each of the 20 agents, as defined in section V-A.2. As an illustration

of META specialty encoding, let's consider that agent R_1 is an aerial vehicle, which has a construction that provides it with a functionality to fight fires on skyscrapers, defined as T_{F_1} in Tables 14 and 15. Its functionality level for this type of task is modulated to 0.8 and defined in its specialty vector, $\boldsymbol{S}_1$, in Table 15. However, the same agent has difficulty fighting fires in large residential complexes, T_{F_2}. This fact can be encoded with a lower functionality level at 0.2 as indicated in Table 15. On the other hand, robot R_2 possesses a functionality which allows it to efficiently act on task T_{F_2} while having lower qualifications for task T_{F_1}. Accordingly, robot R_2 competencies are modulated with a functionality level equal to 0.3 and 0.7 respectively on the corresponding tasks, T_{F_1} and T_{F_2}.

Based on these assumptions and the agents' qualifications defined in Tables 14 and 15, four test cases are analyzed below. All cases consider a low specialty fitting level (*LSFL*) for the task-robot matching process with an enforced MFT level of $\eta = 0.3$.

A. CASE 1: FRAMEWORK VALIDATION WITH HIGH CONFIDENCE IN TARGET OBJECTS DETECTION

This test case considers a high confidence level in the target object detection, here estimated at 0.86, when all of the team members are available for the task assignment. Agents' attendance, Eq. (13), is deactivated considering $\rho = 1$ in Eq. (15) and the task allocation probability is computed by placing full weight on the agents' specialty-based qualification, $\boldsymbol{Q}$, along with the agents' availability status, $\boldsymbol{\vartheta_{Av}}$, in Eq. (12). Fig. 2 illustrates that a target object of type T_{F_1} is detected by a flying robot (shown in red).

The resulting task allocation probabilities for the available robots based on the binary encoding, Eq. (4) and Table 14, are detailed in Table 2 (4^{th} column from the left). Agents R_1,R_2, and R_3 present a specialty fitting score of 0.43 that satisfies the MFT. In addition, agent R_4 presents a lower level of probabilistic fitting of 0.29, which is less than the set MFT (0.3). As a result, this agent, R_4, cannot be allocated to the detected task, T_{F_1}. Therefore, in the case that the system should assign only one agent as the most specialized responder to the detected target, the system, Eq. (19), automatically assigns the first agent in the list among those that have a highest probabilistic fitting level, which is R_1, as depicted in Fig. 2.

On the other hand, when the agents' specializations are modulated in a non-binary form, Eq. (5), as specified in Table 15, the available robots present different levels of probabilistic fitting with respect to the detected task (Table 2, 5^{th} column). In this case, agent R_1 presents the highest specialty fitting probability of 0.69, and agent R_3 presents the second highest value that satisfies the MFT with 0.52.

It is followed by agent R_4 with a level of probabilistic fitting equal to 0.34. All three agents satisfy the MFT and are somewhat qualified for a task of type T_{F_1}. However, agents R_2 presents a specialty fitting probability (0.26) lower than the required MFT. As a result, R_2 cannot be allocated

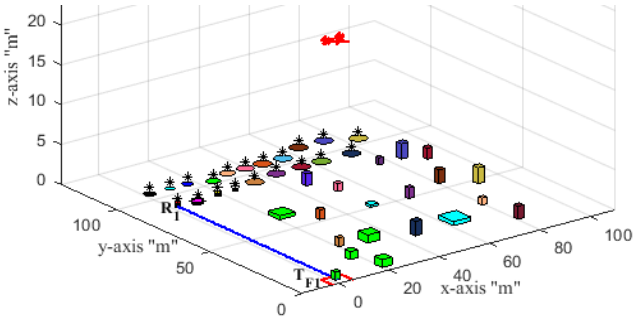

FIGURE 2. Detected target object T_{F_1} and allocation to robot R_1.

to the task (T_{F_1}). Therefore, in the case where the system should assign only one most specialized responder to the detected task, then the system, Eq. (19), automatically assigns the agent with the highest probabilistic fitting, that is R_1. In contrast to the case with binary agents' functionality encoding in which three agents were equally qualified to tackle the detected task, with modulated functionality encoding, the framework provides an increased selectivity on the robot that is best competent to respond to a detected target task.

B. CASE 2: FRAMEWORK VALIDATION WITH AGENTS' AVAILABILITY

When the most qualified agent or agents are ''withdrawn'' or ''busy'', the system must still accomplish the mission goals by substituting the unavailable agents with alternative agents that are currently available and offer adequate functionalities for the task at hand. Considering the proposed availability states, $\boldsymbol{\vartheta}_{Av}$, defined in Eq. (12), the task allocator, Eq. (17), calculates the fitting probabilities of the ''available'' robots. Fig. 3 illustrates another situation from the simulation where a second target object of type T_{E_2} is detected, while all team members are available, as detailed in Table 3(A). In this test case, the binary encoding is considered (Table 14). This time, agents R_{11}, R_{12}, and R_{13} present equal fitting probabilities (0.38), which is above the MFT. Therefore, the system automatically assigns the first agent in the list, R_{11}, to respond to T_{E_2}. However, as this agent R_{11} gets tasked with a mission and becomes unavailable, as indicated in Table 3(B), the system then assigns the next specialized and available agent, R_{12}, to assist the first agent, R_{11}. This test case demonstrates the framework's response when agents' availability is considered along with their specialized binary functionalities (Table 14). Alternatively, when modulated functionalities encoding (Table 15) is considered, the system presents a different response when the same target, T_{E_2}, is detected and all of the team members are initially available. This time, the agents offer different levels of task allocation suitability with respect to the detected task, as detailed in Table 3(A). Agent R_{13} reveals as the most specialized robot with a fitting probability of 0.62, followed by agent R_{12} (0.48).

However, agent R_{11} reaches a lower fitting level of 0.23, which does not satisfy the MFT. As a result, the system

TABLE 2. Specialty-based task allocation dynamics with respect to a task recognized with high confidence level.

Target object class & recognition conf. level	Agent ID#	Task-agent specialty matching probability (ρQ) BETA	Task-agent specialty matching probability (ρQ) META	Agents' availability 1:Available 0:Withdrawn (ϑ_{Av})	Available agents' attendance level ($(1-\rho)\vartheta_{Att}$)	Available qualified agents' fitting probability (Ψ_{MFT}) BETA	Available qualified agents' fitting probability (Ψ_{MFT}) META	MFT (η)
T_{F_1} 0.86	R_1	0.43	0.69	1	---	**0.43***	**0.69***	
	R_2	0.43	0.26	1	---	**0.43**	---	
	R_3	0.43	0.52	1	---	**0.43**	0.52	0.3
	R_4	0.29	0.34	1	---	---	0.34	

* indicates the selected agent allocated to the detected task. **Bold** shows all agents equally qualified for a task.

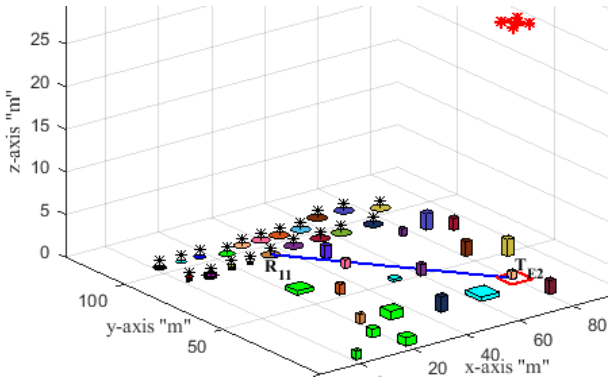

FIGURE 3. Detected target object T_{E_2} inside a red square and allocation to the most specialized agent, R_{11}.

automatically discards agent R_{11} and assigns agent R_{13} to respond to the detected task T_{E_2}. Once agent R_{13} is assigned to allocate the task and becomes unavailable, as shown in Table 3(B), the system pursues the task allocation with the next qualified and available agent, which is R_{12}. This test case demonstrates the validity of the framework's response when agents' availability consideration is combined with a modulated encoding of the agents' specialized functionalities (Table 15). As such, whenever the most specialized agent is not available, the system successfully assigns the next best qualified agent to the detected task. This robust behaviour is not achieved when the agents' specialized functionalities are encoded in a binary form, which confirms the value of modulating the definition of robotic agents' functionalities.

C. CASE 3: PERFORMANCE ANALYSIS UNDER VARIABLE TASK RECOGNITION CONFIDENCE LEVELS

This test case presents comprehensive results for the 14 classes of tasks considered, while assuming that the corresponding target objects would be detected via a deep learning-based recognition stage with a high confidence level in the range of 76-95%. To support this study, a metric to quantitatively monitor the "*agent/task relative robustness*" of the task allocation process is defined. This measure builds upon the modulated specialization level defined in Table 15 as an indicator of the suitability of an agent to perform a task of a specific nature, given the robot's mechanical construction, or onboard embedded hardware or software. This metric is used for quantitative analysis to evaluate the performance of the proposed formulations for the task allocators, BETA and META. Its values are transposed directly from Table 15 to Tables 4 to 7 in the 4th, 7th, 10th and 13th columns of each Table, for every pair of agent/task that is formed. Based on this metric, a colour-coded suitability indicator translates the individual agents' robustness with respect to each task in five categories, those are: 1) The most specialized (green), 2) The second most specialized (blue), 3) The third most specialized (grey), and; 4) The least specialized (orange). In addition, when the task allocation is dropped, the indicator takes the red colour. The results shown in Table 4 correspond to the binary encoding (BETA) of agents' functionalities, defined in Table 14.

Similarly, Table 5 presents the corresponding results when modulated encoding (META) of the agents' functionalities, from Table 15, is used. Furthermore, in order to study the influence of the confidence level from the target objects (task) recognition stage on the proposed task allocation framework.

A complete set of simulations was also conducted with the same candidate agents/tasks, but at a lower recognition confidence level, specifically in the range of 50-60%. Tables 6 and 7 provide a detailed overview of these results. As such, Tables 4, 5, 6, and 7 show four simulated task allocation attempts in response to the detection of each one of the 14 candidate tasks, and while considering either BETA (Table 14) or META (Table 15) encoding of the robotic agents' functionalities. The results are analyzed while considering two types of response for the task allocation operation. The first involves allocating only the most specialized and available agent to a detected task, and the second involves the successive allocation of all qualified agents in descending order of specialization.

1) SINGLE MOST QUALIFIED RESPONDER ASSIGNMENT

In this simulation scenario, the first responder agent must be the most competent and available robotic agent that can respond to the detected task. In Tables 4 and 5, the first responders are listed in the "first assignment" column. Table 4 shows that the first responder in the case of BETA can be selected among different categories of the agent/task relative robustness indicator, as shown by different colours (green, blue, or grey).

This means that in the case of BETA encoding, the proposed task allocator selects a specialized robot to match a detected task regardless the actual level of the agent's

TABLE 3. Specialty-based task allocation dynamics: A) when the most specialized agents are "available".

A) WHEN THE MOST SPECIALIZED AGENTS ARE "AVAILABLE"

Target object class & recognition confidence level		Agent ID#	Task-agent specialty matching probability ($\rho\boldsymbol{Q}$)		Agents' availability 1:Available 0:Withdrawn ($\boldsymbol{\vartheta}_{Av}$)		Available agents' attendance level ($(1-\rho)\boldsymbol{\vartheta}_{Att}$)	Available qualified agents' fitting probability ($\boldsymbol{\Psi}_{MFT}$)		MFT (η)
			BETA	META	BETA	META		BETA	META	
T_{E_2}	0.77	R_{11}	0.38	0.23	**1**	**1**	---	**0.38*1st**	**---**	
		R_{12}	0.38	0.48	**1**	**1**	---	**0.38**	0.48	0.3
		R_{13}	0.38	0.62	**1**	**1**	---	**0.38**	**0.62*1st**	

B) WHEN THE MOST SPECIALIZED AGENTS ARE "WITHDRAWN" OR "BUSY"

T_{E_2}	0.77	R_{11}	0.38	0.23	**0**	**1**	---	---	**---**	
		R_{12}	0.38	0.48	**1**	**1**	---	**0.38*2nd**	**0.48*2nd**	0.3
		R_{13}	0.38	0.62	**1**	**0**	---	**0.38**	**---**	

TABLE 4. Specialty-based task allocation using binary encoded task allocation (beta) with respect to all candidate tasks recognized with a high confidence level (76-95%), and deactivated attendance, MFT (η=0.3).

Task		First Assignment Possibilities			Second Assignment Possibilities			Third Assignment Possibilities			Fourth Assignment Possibilities		
Type	*Recognition Confidence*	*Agent ID#*	*Agent/Task Relative Robustness*	*Task Allocation Probability*	*Agent ID#*	*Agent/Task Relative Robustness*	*Task Allocation Probability*	*Agent ID#*	*Agent/Task Relative Robustness*	*Task Allocation Probability*	*Agent ID#*	*Agent/Task Relative Robustness*	*Task Allocation Probability*
T_{F_1}	0.85	R_1	80%	0.43	R_2	30%	0.43	R_3	60%	0.43	R_4	40%	0.29
T_{F_2}	0.76	R_1	20%	0.38	R_2	70%	0.38	R_5	50%	0.38	R_4	20%	0.29
T_{F_3}	0.87	R_3	40%	0.43	R_5	50%	0.43	R_6	20%	0.43	R_4	40%	0.29
T_{F_4}	0.77	R_6	80%	0.38	R_7	65%	0.38	R_8	50%	0.38			
T_{F_5}	0.95	R_7	35%	0.48	R_8	50%	0.48						
T_{A_1}	0.88	R_9	60%	0.44	R_{10}	40%	0.44						
T_{A_2}	0.90	R_9	40%	0.45	R_{10}	60%	0.45						
T_{E_1}	0.95	R_{11}	70%	0.48	R_{12}	38%	0.48						
T_{E_2}	0.76	R_{11}	30%	0.38	R_{12}	62%	0.38	R_{13}	80%	0.38			
T_{E_3}	0.89	R_{13}	20%	0.45	R_{14}	70%	0.45						
T_{E_4}	0.91	R_{14}	30%	0.46	R_{15}	44%	0.46						
T_{E_5}	0.92	R_{15}	56%	046	R_{16}	36%	0.46	R_{17}	40%	0.46	R_{18}	30%	0.31
T_{E_6}	0.88	R_{16}	64%	0.44	R_{17}	60%	0.44	R_{19}	30%	0.44	R_{18}	30%	0.29
T_{E_7}	0.93	R_{20}	100%	0.93	R_{19}	70%	0.47	R_{18}	30%	0.31			

TABLE 5. Specialty-based task allocation using modulated encoded task allocation (meta) with respect to all candidate tasks recognized with a high confidence level (76-95%), and deactivated attendance, MFT (η=0.3).

Task		First Assignment Possibilities			Second Assignment Possibilities			Third Assignment Possibilities			Fourth Assignment Possibilities		
Type	*Recognition Confidence*	*Agent ID#*	*Agent/Task Relative Robustness*	*Task Allocation Probability*	*Agent ID#*	*Agent/Task Relative Robustness*	*Task Allocation Probability*	*Agent ID#*	*Agent/Task Relative Robustness*	*Task Allocation Probability*	*Agent ID#*	*Agent/Task Relative Robustness*	*Task Allocation Probability*
T_{F_1}	0.85	R_1	80%	0.69	R_3	60%	0.52	R_4	40%	0.34	R_2	30%	0.26
T_{F_2}	0.76	R_2	70%	0.54	R_5	50%	0.38	R_1	20%	0.15	R_4	20%	0.15
T_{F_3}	0.87	R_5	50%	0.44	R_3	40%	0.35	R_4	40%	0.35	R_6	20%	0.18
T_{F_4}	0.77	R_6	80%	0.62	R_7	65%	0.50	R_8	50%	0.38			
T_{F_5}	0.95	R_8	50%	0.48	R_7	35%	0.33						
T_{A_1}	0.88	R_9	60%	0.53	R_{10}	40%	0.35						
T_{A_2}	0.90	R_{10}	60%	0.54	R_9	40%	0.36						
T_{E_1}	0.95	R_{11}	70%	0.67	R_{12}	38%	0.36						
T_{E_2}	0.77	R_{13}	80%	0.62	R_{12}	62%	0.48	R_{11}	30%	0.23			
T_{E_3}	0.89	R_{14}	70%	0.63	R_{13}	20%	0.18						
T_{E_4}	0.91	R_{15}	44%	0.40	R_{14}	30%	0.27						
T_{E_5}	0.92	R_{15}	65%	0.51	R_{17}	40%	0.37	R_{16}	36%	0.33	R_{18}	30%	0.27
T_{E_6}	0.88	R_{16}	64%	0.56	R_{17}	60%	0.52	R_{18}	40%	0.35	R_{19}	30%	0.26
T_{E_7}	0.93	R_{20}	100%	0.31	R_{19}	70%	0.65	R_{18}	30%	0.28			

robustness to tackle that task. This behaviour may result in selecting a first responder agent which is not the most suitable. On the other hand, in the case of META, Table 5 shows that the first responder is systematically selected as the most robust specialized agent (green). With the modulated encoding of functionalities, the proposed task allocator is successful at systematically assigning the most qualified agent from those that also exhibit the highest robustness level to respond to a detected task. In comparison, the performance of BETA in Table 3 is substantially lower. The most qualified and robust responder is selected seven times (green) out of 14.

The responder selection in these seven cases depends on the order in which the agents' probabilistic fitting level is stored in the vector defined in Eq. (17). This interpretation indicates that with BETA, the system can success to assign a specialized agent, but it cannot guarantee that it will be the most robust one. While this may not be entirely desirable, the binary functionalities encoding supported by BETA clearly favors "allocating a resource" over "allocating the best resource" which may prove helpful in circumstances when presence predominates over competence. The response of BETA task allocator is closer to that of classical task allocation frameworks where the specialty of agents is not emphasized while the number of agents, or the response speed represent higher priorities. Conversely, META encoded task allocator introduces a different and innovative perspective to the task allocation problem, where the agents' best resources are prioritized, as demonstrated in Table 6. As a possible severe consequence of BETA, Table 6 exemplifies the case when a lower confidence level is achieved on target recognition (50-60%). BETA fails to respond to all of the detected targets expect in one trial out of the 14 simulated cases. Conversely, Table 7 demonstrates that META still offers a robust performance to allocate the most qualified and robust agents to the detected tasks, succeeding in 11 cases (green) out of the 14 trials.

2) ALL QUALIFIED RESPONDERS ASSIGNMENT

In many applications, such as emergency first responders, a substantial number of agents may be required to manage the situation. Therefore, all qualified agents available within the specific area of a reported incident should be engaged in responding and task allocation. The proposed specialty-based task allocator is designed to accommodate such situations by assigning as many of the available qualified agents as possible who meet the minimum MFT requirement. Considering the simulations described above, in which agent allocation occurs successively after identifying the first responder agent, as discussed in the previous section.

3) COMPARISON

Table 8 consolidates the results from Tables 4, 5, 6, and 7 to provide a comparison between the BETA and META task allocation schemes. The findings of these experiments demonstrate that the BETA task allocator, using binary specialty encoding, prioritizes the allocation of responders with specialized resources when a high confidence level is achieved in target/task detection, rather than considering their speciality-based qualification level or relative robustness. This preference is evident in Table 8, last row, column 2, where 37 successful task allocation processes have been achieved. However, it also highlights a significant susceptibility to failure in agent-task allocation when a lower confidence level is reached in target/task recognition. Table 8, last row, column 4, shows that only one successful task allocation process has been achieved under such conditions, leading to the task allocator encountering uncertainty and struggling to make decisions. On the other hand, the META task allocator, modulating the suitability levels of the agent's specializations, demonstrates greater robustness in dealing with low detection confidence levels and task detection ambiguity, resulting in high-performance allocation for such scenarios. This preference is clear in Table 8, last row, column 5, where 16 successful task allocation processes have been achieved compared to the single case accomplished by BETA under the same task detection conditions. Figure 4 provides graphical illustrations of the distinctions between BETA and META, in terms of the number of successfully allocated specialized agents to tasks detected with both high and low confidence levels, as META reports significant increase in performance compared to BETA especially in difficult cases with low confidence in the target/task detection.

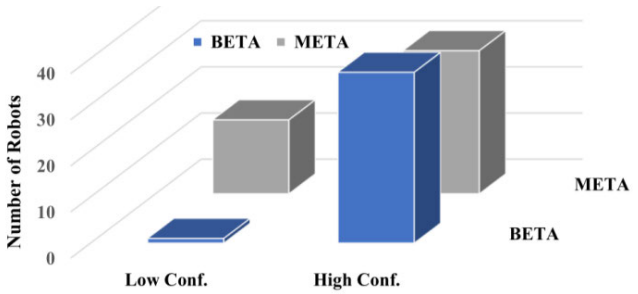

FIGURE 4. Performance comparison between BETA and META.

D. CASE 4: FRAMEWORK VALIDATION WITH AGENTS' ATTENDANCE

In emergency situations, multi-robot coordination plays a prominent role to drive the agents to the locations affected by an incident. For example, let's assume that a heterogeneous firefighting team is distributed over a large-scale city and operates from different fire stations. In total, the team consists of dozens of heterogeneous vehicles, among which some are ground vehicles equipped with different types of equipment, some are aerial vehicles, and others are ambulance vehicles. Initially, they are all distributed over a wide area.

The proposed framework is designed to be responsive to operational conditions involving such wide-range workspace applications. To achieve this purpose, the agents' attendance, $\boldsymbol{\vartheta}_{Att}$, Eq. (13), is activated in Eq. (15) with $\rho < 1$ to optimize the time response of the selected agents to reach the task location where a specific level of services is requested, while continuing to allocate tasks with the specialty-based matching, $\boldsymbol{Q}$, being dependent on the condition that $(1 - \rho) < \eta$.

The purpose of this simulation scenario is to test the adaptability of the proposed approach when the most qualified agent or agents are initially located far away from the target position. While other qualified agents may be closer to the target, the latter might be less competent. In these cases, the system must adapt to control the situation until the arrival of the best suited agents to mitigate injuries and damages. Given that META provides a higher level of efficiency in

TABLE 6. Specialty-based task allocation using binary encoded task allocation (beta) with respect to all candidate tasks recognized with a low confidence level (50-60%), and deactivated attendance, MFT (η=0.3).

Task		First Assignment Possibilities			Second Assignment Possibilities			Third Assignment Possibilities			Fourth Assignment Possibilities		
Type	*Recognition Confidence*	*Agent ID#*	*Agent/Task Relative Robustness*	*Task Allocation Probability*	*Agent ID#*	*Agent/Task Relative Robustness*	*Task Allocation Probability*	*Agent ID#*	*Agent/Task Relative Robustness*	*Task Allocation Probability*	*Agent ID#*	*Agent/Task Relative Robustness*	*Task Allocation Probability*
T_{F_1}	0.58	R_1	80%	0.29	R_2	30%	0.29	R_3	60%	0.29	R_4	40%	0.19
T_{F_2}	0.56	R_1	20%	0.28	R_2	70%	0.28	R_5	50%	0.28	R_4	20%	0.19
T_{F_3}	0.56	R_3	40%	0.28	R_5	50%	0.28	R_6	20%	0.28	R_4	40%	0.19
T_{F_4}	0.56	R_6	80%	0.28	R_7	65%	0.28	R_8	50%	0.28			
T_{F_5}	0.56	R_7	35%	0.28	R_8	50%	0.28						
T_{A_1}	0.56	R_9	60%	0.28	R_{10}	40%	0.28						
T_{A_2}	0.56	R_9	40%	0.28	R_{10}	60%	0.28						
T_{E_1}	0.56	R_{11}	70%	0.28	R_{12}	38%	0.28						
T_{E_2}	0.56	R_{11}	30%	0.28	R_{12}	62%	0.28	R_{13}	80%	0.28			
T_{E_3}	0.56	R_{13}	20%	0.28	R_{14}	70%	0.28						
T_{E_4}	0.56	R_{14}	30%	0.28	R_{15}	44%	0.28						
T_{E_5}	0.56	R_{15}	56%	0.28	R_{16}	36%	0.28	R_{17}	40%	0.28	R_{18}	30%	0.18
T_{E_6}	0.56	R_{16}	64%	0.28	R_{17}	60%	0.28	R_{19}	30%	0.28	R_{18}	30%	0.18
T_{E_7}	0.56	R_{20}	100%	0.56	R_{19}	70%	0.28	R_{18}	30%	0.18			

TABLE 7. Specialty-based task allocation using modulated encoded task allocation (meta) with respect to all candidate tasks recognized with a low confidence level (50-60%), and deactivated attendance, MFT (η=0.3).

Task		First Assignment Possibilities			Second Assignment Possibilities			Third Assignment Possibilities			Fourth Assignment Possibilities		
Type	*Recognition Confidence*	*Agent ID#*	*Agent/Task Relative Robustness*	*Task Allocation Probability*	*Agent ID#*	*Agent/Task Relative Robustness*	*Task Allocation Probability*	*Agent ID#*	*Agent/Task Relative Robustness*	*Task Allocation Probability*	*Agent ID#*	*Agent/Task Relative Robustness*	*Task Allocation Probability*
T_{F_1}	0.58	R_1	80%	0.46	R_3	60%	0.35	R_4	40%	0.23	R_2	30%	0.17
T_{F_2}	0.56	R_2	70%	0.39	R_5	50%	0.28	R_1	20%	0.11	R_4	20%	0.11
T_{F_3}	0.56	R_5	50%	0.28	R_3	40%	0.22	R_4	40%	0.22	R_6	20%	0.11
T_{F_4}	0.56	R_6	80%	0.44	R_7	65%	0.36	R_8	50%	0.28			
T_{F_5}	0.56	R_8	50%	0.28	R_7	35%	0.19						
T_{A_1}	0.56	R_9	60%	0.34	R_{10}	40%	0.22						
T_{A_2}	0.56	R_{10}	60%	0.34	R_9	40%	0.22						
T_{E_1}	0.56	R_{11}	70%	0.39	R_{12}	38%	0.21						
T_{E_2}	0.56	R_{13}	80%	0.45	R_{12}	62%	0.34	R_{11}	30%	0.17			
T_{E_3}	0.56	R_{14}	70%	0.39	R_{13}	20%	0.11						
T_{E_4}	0.56	R_{15}	44%	0.25	R_{14}	30%	0.17						
T_{E_5}	0.56	R_{15}	65%	0.31	R_{17}	40%	0.22	R_{16}	36%	0.20	R_{18}	30%	0.17
T_{E_6}	0.56	R_{16}	64%	0.36	R_{17}	60%	0.34	R_{19}	40%	0.22	R_{18}	30%	0.17
T_{E_7}	0.56	R_{20}	100%	0.56	R_{19}	70%	0.39	R_{18}	30%	0.17			

comparison with BETA, as demonstrated in previous test cases, simulation in this scenario is conducted with the modulated encoding of agents' functionalities only.

Assumptions are made to mimic the properties of a realistic first responder system in the simulated trials. First, the average velocity of all ground vehicle agents is assumed to be 50 km/hour. For robots that have higher velocity as one of their specialized attribute, such as aerial vehicles, this attribute is weighted in the corresponding robots' modulated specialty encoding vector (Table 15). The Euclidean distance represents the travelling distance that separates the robot from the target's location. In addition, a static target is considered for the robots' attendance state, Eq. (14), that results in $\epsilon = 0$ and $v_t < v_{max}$. The latter leads to $\bar{\mathrm{T}} = 1$.

Fig. 5 illustrates a similar situation to the one that has been considered in the test case 1 above (shown in Fig. 2), where a task of type T_{F_1} is detected with a confidence level equal to 0.86, while all of the team members are available. However, the scale of the problem is expanded with the agents and tasks being distributed over a wider area to test the scaling problem of interest in this case. The system, in test case 1 above, processes the agents' probabilistic fitting levels based on Eqs. (17) and (19) to respond to the detected task. The matching probabilities of the specialized available team members shown in Table 8 are computed with deactivated attendance, $\boldsymbol{\vartheta}_{Att}$, that is with $\rho = 1$ for comparison purposes. Agents R_1, R_3, and R_4 present fitting probabilities above the MFT. According to Table 8, the distances separating the agents R_1, R_3, and R_4 from the target location are 78 *km*, 23.9 *km*, and 25.6 *km* respectively. Although agent R_2 is located closer to the target location (14.1 *km* away), this agent is not minimally qualified to respond to the current task because it does not achieve the MFT (set to 0.3). Similar to test case 3 above, two types of response for the task allocation process are analyzed here, one involving only the most specialized and available agent, the other involving all qualified agents.

1) SINGLE MOST QUALIFIED RESPONDER ASSIGNMENT

When only the most qualified agent is considered, that is agent R_1 which is located 78 *km* away from the target location, it would require approximately 94 minutes to arrive at the scene with the set average speed. This can represent a

TABLE 8. Successful task allocation possibilities/task when all qualified agents must be allocated to the detected task.

Task	High confidence level of target object detection:		Low confidence level of target object detection:	
	BETA (Table 4)	META (Table 5)	BETA (Table 6)	META (Table 7)
	Number of successful responders per Task	Number of successful responders per Task	Number of successful responders per Task	Number of successful responders per Task
T_{F_1}	3	3	Failed	2
T_{F_2}	3	2	Failed	1
T_{F_3}	3	3	Failed	Failed
T_{F_4}	3	3	Failed	2
T_{F_5}	2	2	Failed	Failed
T_{A_1}	2	2	Failed	1
T_{A_2}	2	2	Failed	1
T_{E_1}	2	2	Failed	1
T_{E_2}	3	2	Failed	2
T_{E_3}	2	1	Failed	1
T_{E_4}	2	1	Failed	Failed
T_{E_5}	4	3	Failed	1
T_{E_6}	3	3	Failed	2
T_{E_7}	3	2	1	2
Total	**37**	**31**	**1**	**16**

weakness of the task allocation framework for wide-range workspace applications. However, when agents' attendance, ϑ_{Att}, is activated in Eq. (15) with $\rho < 1$, then the system generates a different response, as shown in Fig. 5. It then assigns a closer agent, R_3, as a first responder to T_{F_1}, as detailed in Table 9. Being initially closer to the task, agent R_3 can reach the scene within 29 minutes while still providing a relatively high level of competency (60% agent/task robustness versus 80% for R_1). This example demonstrates the purpose and benefit of giving consideration to attendance in the proposed task allocation framework.

2) ALL QUALIFIED RESPONDERS ASSIGNMENT

If more than one agent are to be assigned on a task, Table 9 indicates that the qualified responders are R_1, R_3, and R_4. Without attendance, the closest responders, R_3 and R_4, can reach the task location within 29 and 31 minutes respectively. The possibility to assign agent R_2 is dropped. On the other hand, when the agents' attendance is activated, the system exhibits a different response and automatically preserves agent R_2 as a candidate given that it is located closer to the task and can intervene faster, in spite of possessing substantially lower qualifications. Agent R_2 can reach the task much faster than the other more specialized agents, that is within 17 minutes, as indicated in Table 10. As a result, the system capacity is increased from three to four qualified responders and the time of first arrival is substantially reduced. This example demonstrates the flexibility embedded in the proposed framework to balance the need for specialized functionalities with the benefits of efficient proactive response of the task allocator in complex scenarios. Table 11 summarizes the observations regarding the influence of agents' attendance as part of the task allocation process. For applications that prioritize the allocation of only one qualified agent to a given task, agents attendance improves the system's response by selecting an alternative agent that can response faster while not significantly degrading competency. On the other hand, for applications that require the intervention of all qualified agents in the shortest possible time, agents' attendance increases the capacity of the system by preserving agents in close proximity and extending the overall number of agents that can respond. The framework then automatically articulates a blend of fast and competent responders. As a result, the consideration of agents' attendance extends and strengthens the application of the proposed specialty-based task allocation framework to swarms of robots distributed over wide workspaces.

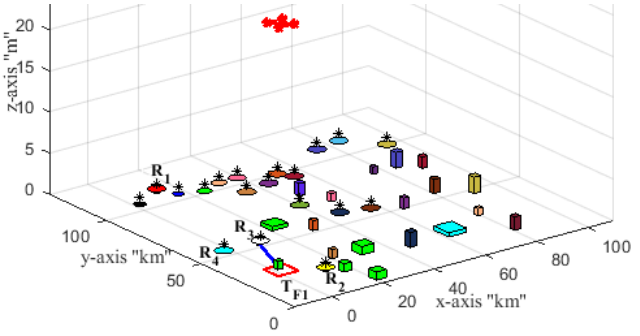

FIGURE 5. Task T_{F_1} allocated to a closer robot R_3 over a wide range workspace, with activated attendance in Eq. (15).

VIII. EXPERIMENTS ON PHYSICAL ROBOTS

To validate the feasibility of the proposed approach for its real-life applications, experiments are conducted on real robotic platforms.

A. EXPERIMENTAL SETUP

To accomplish this, a multi-agent robotic system was deployed using two different physical platforms: the TurtleBot3 (Burger) and another TurtleBot3 (Waffle Pi) [40], [41].

To conduct this test case and considering the availability of robotic agents, the proposed framework is examined in this section by introducing a third virtual robotic agent named "Milkshake" which is assumed to be unavailable ("withdrawn" state). The experimental configuration utilizes a laptop equipped with a central processing unit (CPU) running the Linux (Ubuntu) operating system. This laptop also runs a ROS navigation stack to facilitate communication between the system components, the later consists of: 1) ATSU, which runs on the CPU as a high-level primary node, managing interaction among the nodes and handles the proposed task allocation process to compute the agents fitting levels based on detected target objects. 2) The low-level sensors and actuators of the robotic agents, each equipped with a Raspberry Pi microcomputer board. The Raspberry Pi connects to the OpenCR via wired communication and maintains a wireless link with the central controller. The OpenCR is the agent's local microcontroller, executing commands that are received

TABLE 9. Specialty-based task allocation with a deactivated attendance, $\rho = 1$ in Eq. 15. MFT (η=0.3), $v_i = 50km/hr$.

Target object class & recognition confidence level	Agent		Task-agent specialty matching probability ($\rho\boldsymbol{Q}$)	Agents' availability 1:Available 0:Withdrawn ($\boldsymbol{\vartheta}_{Av}$)	Available agents' attendance level $(1-\rho)\boldsymbol{\vartheta}_{Att}$	Available qualified agents' fitting probability ($\boldsymbol{\Psi}_{MFT}$)	Agent to target travelling distance $(d_i)Km$	Qualified Responders	
	ID#	Agent/Task relative robustness	META					Order	Time of arrival (min.)
T_{F_1} 0.86	$\boldsymbol{R_1}$	**80%**	**0.69**	**1**	---	**0.69***	**78**	**1st**	**94**
	R_2	30%	0.26	1	---	---	14.1	Dropped	17
	R_3	60%	0.52	1	---	0.52*	23.9	2nd	29
	R_4	40%	0.34	1	---	0.34*	25.6	3rd	31

TABLE 10. Specialty-based task allocation with activated attendance, $\rho = 1-(\eta-0.1)$ in Eq. (15), MFT (η=0.3) $v_i = 50km/hr$.

Target object class & recognition confidence level	Agent		Task-agent specialty matching probability ($\rho\boldsymbol{Q}$)	Agents' availability 1:Available 0:Withdrawn ($\boldsymbol{\vartheta}_{Av}$)	Available Agents' attendance level $((1-\rho)\boldsymbol{\vartheta}_{Att})$	Available qualified agents fitting probability ($\boldsymbol{\Psi}_{MFT}$)	Agent to target travelling distance $(d_i)Km$	Qualified Responders	
	ID#	Agent/Task relative robustness	META					Order	Time of arrival (min.)
T_{F_1} 0.86	R_1	80%	0.48	1	0.05	0.53*	78.0	2nd	94
	R_2	30%	0.18	1	0.29	0.47*	14.1	3rd	17
	$\boldsymbol{R_3}$	**60%**	**0.36**	**1**	**0.18**	**0.54***	**23.9**	**1st**	**29**
	R_4	40%	0.24	1	0.17	0.41*	25.4	4th	31

TABLE 11. System performance in presence of agents attendance.

Attendance	Most qualified agent		All qualified agents	
	Time of arrival of the selected agent (minutes)	Agent/task relative robustness	Time of arrival of the first agent (minutes)	System's capacity
Deactivated	94	80%	29	(3 agents) 75%
Activated	29	60%	17	(4 agents) 100%
Observations	**65 (min) earlier**	**20% lower**	**12 (min) earlier**	**Increased with 25%**

from the central controller (ATSU) through the Raspberry Pi to drive the robots low-level servo motors. It also gathers pose data from the odometer sensors and directly connects to the ATSU through the Raspberry Pi. 3) The communication link is established via a shared Wi-Fi network broadcast by a smartphone device. ROS network enables information and command exchange between the robotic agent's local controller (the OpenCR) and the central controller (ATSU), as well as the target object detection unit. Programming of the OpenCR microcontroller is performed using the Arduino IDE.

B. TARGET TASK DETECTION

The experiments are conducted taking into account three tasks represented as target objects placed within the workspace. Each object is a cylindrical shape with a specific combination of two vertically adjacent color features: red-green, red-blue, and green-blue, respectively. Each color combination represents a specific class of a task associated with one of the specialized robotic agents, while the other robotic agents can provide varying levels of qualification to respond to the same target object. Considering the nature of the tasks in these experiments, the corresponding robots specialization vectors, denoted as $\boldsymbol{S_i}$, are formulated in a specific format that supports both binary and modulated functionality

TABLE 12. Robotic agents' specialization coding for experiments with real robots.

Agent name	0.5=Possesses functionality; 0 = Does not possess functionality			
	Specialty vector	Red feature	Blue feature	Green feature
Burger	$\boldsymbol{S_1}$	0.5	0	0.5
Waffle Pi	$\boldsymbol{S_2}$	0.5	0.5	0
Milkshake	$\boldsymbol{S_3}$	0	0.5	0.5

encoding, as defined in Table 12. In these experiments, a color sensor, specifically the E-con Systems' See3CAM_130 USB 3.1 camera [39], is employed to detect the features on a target object. The recognition stage utilizes an 8-bit Hue-Saturation-Value (HSV) color space representation, which is employed to classify the target objects into specific tasks falling under the defined three categories. Based on the observations from the experiments, each colour can be detected within a range of ± 5 units around its hue value. To make use of these uncertain color detection results, the following formula is derived to calculate the confidence level for task class recognition:

$$P_{C_l} = \frac{10 - [actual\ hue - |detected\ hue|]}{10} \tag{20}$$

To facilitate integration with the task allocation stage, the output of the task features classification stage, as per

TABLE 13. Specialized physical agents' matching probabilities with respect to a target of class red-green.

Target object features recognition confidence level	Agent name	Task-agent specialty matching probability ($\rho \boldsymbol{Q}$) BETA/META	Agents' Availability 1:Available 0:Withdrawn ($\boldsymbol{\vartheta}_{Av}$)	Available agents' attendance level ($\boldsymbol{\vartheta}_{Att}$)	Available qualified agents' fitting probability ($\boldsymbol{\Psi}_{MFT}$)	MFT (η)
Red: 0.70 Blue: 0.00 Green: 0.80	Burger	0.75	1	---	0.75*	0.3
	Waffle Pi	0.35	1	---	0.00	
	Milkshake	0.40	0	---	0.00	

TABLE 14. Formulation of $M = 20$ robotic agents with binary encoded specialization functionalities to serve on 14 tasks with different requirements illustrated in the context of a robotic team coordination.

Agents' specialization binary vectors	e.g. Firefighting Tasks					e.g. Ambulance Tasks		e.g. External Threats (Defense Tasks)						
	T_{F_1}	T_{F_2}	T_{F_3}	T_{F_4}	T_{F_5}	T_{A_1}	T_{A_2}	T_{E_1}	T_{E_2}	T_{E_3}	T_{E_4}	T_{E_5}	T_{E_6}	T_{E_7}
$\boldsymbol{S_1}$	1	1	0	0	0	0	0	0	0	0	0	0	0	0
$\boldsymbol{S_2}$	1	1	0	0	0	0	0	0	0	0	0	0	0	0
$\boldsymbol{S_3}$	1	0	1	0	0	0	0	0	0	0	0	0	0	0
$\boldsymbol{S_4}$	1	1	1	0	0	0	0	0	0	0	0	0	0	0
$\boldsymbol{S_5}$	0	1	1	0	0	0	0	0	0	0	0	0	0	0
$\boldsymbol{S_6}$	0	0	1	1	0	0	0	0	0	0	0	0	0	0
$\boldsymbol{S_7}$	0	0	0	1	1	0	0	0	0	0	0	0	0	0
$\boldsymbol{S_8}$	0	0	0	1	1	0	0	0	0	0	0	0	0	0
$\boldsymbol{S_9}$	0	0	0	0	0	1	1	0	0	0	0	0	0	0
$\boldsymbol{S_{10}}$	0	0	0	0	0	1	1	0	0	0	0	0	0	0
$\boldsymbol{S_{11}}$	0	0	0	0	0	0	0	1	1	0	0	0	0	0
$\boldsymbol{S_{12}}$	0	0	0	0	0	0	0	1	1	0	0	0	0	0
$\boldsymbol{S_{13}}$	0	0	0	0	0	0	0	0	1	1	0	0	0	0
$\boldsymbol{S_{14}}$	0	0	0	0	0	0	0	0	0	1	1	0	0	0
$\boldsymbol{S_{15}}$	0	0	0	0	0	0	0	0	0	0	1	1	0	0
$\boldsymbol{S_{16}}$	0	0	0	0	0	0	0	0	0	0	0	1	1	0
$\boldsymbol{S_{17}}$	0	0	0	0	0	0	0	0	0	0	0	1	1	0
$\boldsymbol{S_{18}}$	0	0	0	0	0	0	0	0	0	0	0	1	1	1
$\boldsymbol{S_{19}}$	0	0	0	0	0	0	0	0	0	0	0	0	1	1
$\boldsymbol{S_{20}}$	0	0	0	0	0	0	0	0	0	0	0	0	0	1

Equation (7), is reformulated as follows:

$$\hat{\boldsymbol{P}}_T = \left[P_{C_1}, P_{C_2}, P_{C_3}\right]^T \tag{21}$$

where C_l:$l = 1:3$ denote the used colour features that are red, blue, and green respectively. P_{C1}∼P_{C3} is the recognition confidence level on a target object associated with each class of tasks identified by a pair of colours.

C. DISCUSSION

In the conducted test cases with real robots, as depicted in Fig. 6a, the multi-agent system comprises two physically available robotic platforms: the Burger robot on the right and the Waffle-Pi robot on the left, along with a virtual ''withdrawn'' agent named Milkshake. For clarity, each available robotic agent is equipped with a top-mounted colored tag that corresponds to the target/task category (class) to which the agent is best qualified to be assigned. Upon initialization, the team navigates the workspace and scans for target objects using their embedded cameras. Fig. 6 depicts the team's mission at various stages of the task allocation process, starting from the initiation and progressing to task completion.

A target object associated with a task in the red-green category is detected. It is best matching with the functionalities of the Burger robot (on the right) based on the agents' specialization encoding defined in Table 12.

The task allocation process computes the agent's matching probability using Eqs. (19) and considering $\rho = 1$ in Eq. (15). Agents' attendance is deactivated given that the experiments are performed in an indoor lab environment over a limited operational workspace area. This configuration places the entire computational load of determining the overall task allocation probability on the agents' specialty-based qualification, denoted as $\boldsymbol{Q}$. The experiment focuses on evaluating the task allocation operation based on the fundamental component of the proposed framework, which is the alignment between the agents' specialized capabilities and the task's specific constraints.

Table 13 presents the complete results for this test case, including the individual agents' availability status, and the task-agent matching probabilities. The results from real experiments demonstrate that the proposed framework performs as expected when transposed onto an implementation with a group of specialized physical robotic agents.

TABLE 15. Formulation of $M = 20$ robotic agents with modulated encoding of different levels of specialization functionalities to serve on 14 tasks with different requirements illustrated in the context of a robotic team coordination.

Agents' specialization modulated vectors	e.g. Firefighting Tasks					e.g. Ambulance Tasks		e.g. External Threats (Defense Tasks)						
	T_{F_1}	T_{F_2}	T_{F_3}	T_{F_4}	T_{F_5}	T_{A_1}	T_{A_2}	T_{E_1}	T_{E_2}	T_{E_3}	T_{E_4}	T_{E_5}	T_{E_6}	T_{E_7}
S_1	0.8	0.2	0	0	0	0	0	0	0	0	0	0	0	0
S_2	0.3	0.7	0	0	0	0	0	0	0	0	0	0	0	0
S_3	0.6	0	0.4	0	0	0	0	0	0	0	0	0	0	0
S_4	0.4	0.2	0.4	0	0	0	0	0	0	0	0	0	0	0
S_5	0	0.5	0.5	0	0	0	0	0	0	0	0	0	0	0
S_6	0	0	0.2	0.8	0	0	0	0	0	0	0	0	0	0
S_7	0	0	0	0.65	0.35	0	0	0	0	0	0	0	0	0
S_8	0	0	0	0.5	0.5	0	0	0	0	0	0	0	0	0
S_9	0	0	0	0	0	0.6	0.4	0	0	0	0	0	0	0
S_{10}	0	0	0	0	0	0.4	0.6	0	0	0	0	0	0	0
S_{11}	0	0	0	0	0	0	0	0.7	0.3	0	0	0	0	0
S_{12}	0	0	0	0	0	0	0	0.38	0.62	0	0	0	0	0
S_{13}	0	0	0	0	0	0	0	0	0.8	0.2	0	0	0	0
S_{14}	0	0	0	0	0	0	0	0	0	0.7	0.3	0	0	0
S_{15}	0	0	0	0	0	0	0	0	0	0	0.44	0.56	0	0
S_{16}	0	0	0	0	0	0	0	0	0	0	0	0.36	0.64	0
S_{17}	0	0	0	0	0	0	0	0	0	0	0	0.4	0.6	0
S_{18}	0	0	0	0	0	0	0	0	0	0	0	0.3	0.4	0.3
S_{19}	0	0	0	0	0	0	0	0	0	0	0	0	0.3	0.7
S_{20}	0	0	0	0	0	0	0	0	0	0	0	0	0	1

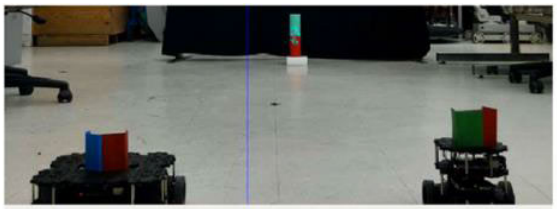

(a) t=0 sec.: Searching for target.

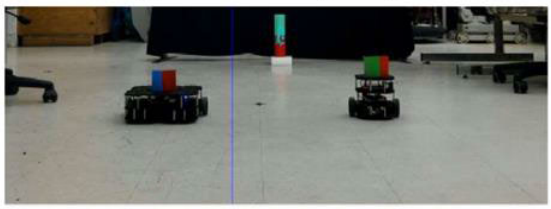

(b) t = 15 sec.: Searching for target.

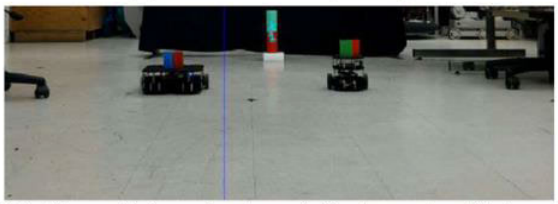

(c) t = 21 sec.: Task zone border, assigning the most qualified agent.

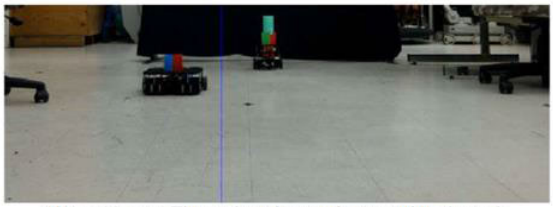

(d) t = 32 sec.: The assigned agent is executing the task.

FIGURE 6. Specialized agents search for a target, reach it, and complete the task.

IX. CONCLUSION

This paper addresses the design aspects of a task allocation framework for a swarm of heterogeneous robotic agents in terms of the agents' specialization. The specialized functionalities of individual robotic agents, such as specific mechanical or instrumentation characteristics embedded on heterogeneous robotic agents, are modeled in two forms. First, a binary definition of agents' specialization (BETA) is introduced as basis for robot-task matching process. Then, a modulated definition (META) of the agents' specialization is proposed as a refined representation of suitability level of the robotic agents' qualifications to perform different tasks, which increases the task allocation possibilities especially when the targets are detected with low confidence. The reported case in Table 8 indicates that META outperforms BETA by 16 times. The specialized functionalities of individual robotic agents are matched to corresponding classes of visually detected features that support recognition of target objects with a quantified confidence level. The latter is used to tune a novel task-agent probabilistic matching scheme which computes the overall specialty-based task allocation probability of the individual agents. The framework then automatically assigns the qualified agents to corresponding tasks. Considering the agents' availability state and attendance level increases the system capacity by 25% as indicated in the tested cases, while they significantly reduce the task allocation time as indicated in Table 11, which can effectively deal with workspaces of various sizes. Simulation experiments demonstrate that the proposed approach is efficient, flexible and reliable for properly assigning specialized agents to corresponding tasks. Experiments with physical ground robots also confirm the viability of the proposed framework for a variety of autonomous robotic applications.

The test results indicate a significant increase in the performance of the proposed approach when the suitability levels of the agent's specializations are adopted for the task allocation process. However, during the design and implementation of

the proposed framework, several constraints have been considered, including a simulated sensing layer, offline object detection input, as well as a well-structured laboratory testing environment. Alternatively, it will be a very interesting future direction to integrate the proposed framework with an advanced sensing layer for online measurements of task characteristics. Furthermore, it is important to study complex tasks in a complex environment, aligning the proposed framework to its greatest extent with real-life applications. Additionally, the human operator contributes to the system's situational understanding through intervention in the MFT set point. However, challenges arise with larger numbers of robots and increasing task requests, which can pose potential difficulties for the operator. Therefore, there is an opportunity to enhance system reasoning to reduce human cognitive load and accommodate a growing number of autonomous robots.

ACKNOWLEDGMENT

The authors would like to thank Paulo Vitor Do Canto Cardoso for his assistance with performing validation on physical robots.

APPENDIX

See Tables 14 and 15.

REFERENCES

[1] M. Rossi and D. Brunelli, "Autonomous gas detection and mapping with unmanned aerial vehicles," *IEEE Trans. Instrum. Meas.*, vol. 65, no. 4, pp. 765–775, Apr. 2016.

[2] T. Tomic, K. Schmid, P. Lutz, A. Domel, M. Kassecker, E. Mair, I. L. Grixa, F. Ruess, M. Suppa, and D. Burschka, "Toward a fully autonomous UAV: Research platform for indoor and outdoor urban search and rescue," *IEEE Robot. Autom. Mag.*, vol. 19, no. 3, pp. 46–56, Sep. 2012.

[3] A. Fahim and Y. Gadallah, "An optimized LTE-based technique for drone base station dynamic 3D placement and resource allocation in delay-sensitive M2M networks," *IEEE Trans. Mobile Comput.*, vol. 22, no. 2, pp. 732–743, Feb. 2023.

[4] C. Friedrich, A. Lechler, and A. Verl, "Autonomous systems for maintenance tasks—Requirements and design of a control architecture," *Proc. Technol.*, vol. 15, pp. 595–604, Jan. 2014.

[5] J. J. Q. Yu, "Two-stage request scheduling for autonomous vehicle logistic system," *IEEE Trans. Intell. Transp. Syst.*, vol. 20, no. 5, pp. 1917–1929, May 2019.

[6] M. P. Manuel, M. Faied, M. Krishnan, and M. Paulik, "Robot platooning strategy for search and rescue operations," *Intell. Service Robot.*, vol. 15, no. 1, pp. 57–68, Mar. 2022.

[7] R. D. Brown-Gaston and A. S. Arora, "War and peace: Ethical challenges and risks in military robotics," *Int. J. Intell. Inf. Technol.*, vol. 17, no. 3, pp. 1–12, Jul. 2021.

[8] O. Al-Buraiki and P. Payeur, "Task allocation in multi-robot systems based on the suitability level of the individual agents," in *Proc. IEEE 17th Int. Conf. Autom. Sci. Eng. (CASE)*, Lyon, France, Aug. 2021, pp. 209–214.

[9] K. J. O'Hara and T. R. Balch, "*Pervasivesensor – less* networks for cooperative multi-robot tasks," in *Distributed Autonomous Robotic Systems*, vol. 6. Tokyo, Japan: Springer, 2007, pp. 305–314.

[10] N. Mathews, A. L. Christensen, R. O'Grady, and M. Dorigo, "Spatially targeted communication and self-assembly," in *Proc. IEEE/RSJ Int. Conf. Intell. Robots Syst.*, Oct. 2012, pp. 2678–2679.

[11] A. Sadeghi and S. L. Smith, "Heterogeneous task allocation and sequencing via decentralized large neighborhood search," *Unmanned Syst.*, vol. 5, no. 2, pp. 79–95, Apr. 2017.

[12] A. J. Ijspeert, A. Martinoli, A. Billard, and L. M. Gambardella, "Collaboration through the exploitation of local interactions in autonomous collective robotics: The stick pulling experiment," *Auto. Robots*, vol. 11, no. 2, pp. 149–171, 2001.

[13] M. A. Hsieh, A. Halasz, E. D. Cubuk, S. Schoenholz, and A. Martinoli, "Specialization as an optimal strategy under varying external conditions," in *Proc. IEEE Int. Conf. Robot. Autom.*, May 2009, pp. 1941–1946.

[14] A. M. Halász, Y. Liang, M. A. Hsieh, and H. J. Lai, "Emergence of specialization in a swarm of robots," in *Distributed Autonomous Robotic Systems*. Berlin, Germany: Springer, 2013, pp. 403–416.

[15] G. Pini, A. Brutschy, A. Scheidler, M. Dorigo, and M. Birattari, "Task partitioning in a robot swarm: Object retrieval as a sequence of subtasks with direct object transfer," *Artif. Life*, vol. 20, no. 3, pp. 291–317, Jul. 2014.

[16] E. Buchanan, A. Pomfret, and J. Timmis, "Dynamic task partitioning for foraging robot swarms," in *Proc. Int. Conf. Swarm Intell.* Cham, Switzerland: Springer, 2016, pp. 113–124.

[17] P. Trueba, A. Prieto, F. Bellas, P. Caamaño, and R. J. Duro, "Specialization analysis of embodied evolution for robotic collective tasks," *Robot. Auto. Syst.*, vol. 61, no. 7, pp. 682–693, Jul. 2013.

[18] J.-M. Montanier, S. Carrignon, and N. Bredeche, "Behavioral specialization in embodied evolutionary robotics: Why so difficult" *Frontiers Robot. AI*, vol. 3, p. 38, Jul. 2016.

[19] H.-L. Choi, L. Brunet, and J. P. How, "Consensus-based decentralized auctions for robust task allocation," *IEEE Trans. Robot.*, vol. 25, no. 4, pp. 912–926, Aug. 2009.

[20] S. L. Smith and F. Bullo, "Target assignment for robotic networks: Worst-case and stochastic performance in dense environments," in *Proc. 46th IEEE Conf. Decis. Control*, Dec. 2007, pp. 3585–3590.

[21] T. Lang and M. Toussaint, "Relevance grounding for planning in relational domains," in *Proc. Joint Eur. Conf. Mach. Learn. Knowl. Discovery Databases*. Berlin, Germany: Springer, Sep. 2009, pp. 736–751.

[22] M. Toussaint, N. Plath, T. Lang, and N. Jetchev, "Integrated motor control, planning, grasping and high-level reasoning in a blocks world using probabilistic inference," in *Proc. IEEE Int. Conf. Robot. Autom.*, May 2010, pp. 385–391.

[23] T. Yasuda, K. Kage, and K. Ohkura, "Response threshold-based task allocation in a reinforcement learning robotic swarm," in *Proc. IEEE 7th Int. Workshop Comput. Intell. Appl. (IWCIA)*, Nov. 2014, pp. 189–194.

[24] H. Ravichandar, K. Shaw, and S. Chernova, "STRATA: Unified framework for task assignments in large teams of heterogeneous agents," *Auto. Agents Multi-Agent Syst.*, vol. 34, no. 2, pp. 1–25, Oct. 2020.

[25] J. C. Amorim, V. Alves, and E. P. de Freitas, "Assessing a swarm-GAP based solution for the task allocation problem in dynamic scenarios," *Expert Syst. Appl.*, vol. 152, Aug. 2020, Art. no. 113437.

[26] E. Czatnecki and A. Dutta, "Hedonic coalition formation for task allocation with heterogeneous robots," in *Proc. IEEE Int. Conf. Syst., Man Cybern. (SMC)*, Oct. 2019, pp. 1024–1029.

[27] O. Al-Buraiki and P. Payeur, "Probabilistic task assignment for specialized multi-agent robotic systems," in *Proc. IEEE Int. Symp. Robotic Sensors Environ. (ROSE)*, Jun. 2019, pp. 1–7.

[28] O. Al-Buraiki, W. Wu, and P. Payeur, "Probabilistic allocation of specialized robots on targets detected using deep learning networks," *Robotics*, vol. 9, no. 3, p. 54, Jul. 2020.

[29] A. Brutschy, G. Pini, C. Pinciroli, M. Birattari, and M. Dorigo, "Self-organized task allocation to sequentially interdependent tasks in swarm robotics," *Auto. Agents Multi-Agent Syst.*, vol. 28, no. 1, pp. 101–125, Jan. 2014.

[30] M. Kulich, J. Faigl, and L. Preucil, "On distance utility in the exploration task," in *Proc. IEEE Int. Conf. Robot. Autom.*, May 2011, pp. 4455–4460.

[31] M. Ross, P. Payeur, and S. Chartier, "Task allocation for heterogeneous robots using a self-organizing contextual map," in *Proc. IEEE Int. Symp. Robotic Sensors Environ. (ROSE)*, Jun. 2019, pp. 1–6.

[32] O. Al-Buraiki, P. Payeur, and Y. R. Castillo, "Task switching for specialized mobile robots working in cooperative formation," in *Proc. IEEE Int. Symp. Robot. Intell. Sensors (IRIS)*, Tokyo, Japan, Dec. 2016, pp. 207–212.

[33] C. M. Bishop, *Pattern Recognition and Machine Learning*. New York, NY, USA: Springer, 2016.

[34] W. Wu, P. Payeur, O. Al-Buraiki, and M. Ross, "Vision-based target objects recognition and segmentation for unmanned systems task allocation," in *Image Analysis and Recognition* (Lecture Notes in Computer Science), vol. 11662, F. Karray, A. Campilho, and A. Yu, Eds. Cham, Switzerland: Springer, 2019, pp. 252–263.
[35] A. Papoulis and S. U. Pillai, *Probability—Random Variables, and Stochastic Processes*. New York, NY, USA: McGraw-Hill, 2002.
[36] O. Al-Buraiki and P. Payeur, "Agent-task assignation based on target characteristics for a swarm of specialized agents," in *Proc. IEEE Int. Syst. Conf. (SysCon)*, Apr. 2019, pp. 268–275.
[37] R. Murphy and J. Burke, "The safe human–robot ratio," in *Human-Robot Interactions in Future Military Operations*. Boca Raton, FL, USA: CRC Press, 2016, pp. 51–70.
[38] L. G. Weiss, "Autonomous robots in the fog of war," *IEEE Spectr.*, vol. 48, no. 8, pp. 30–57, Aug. 2011.
[39] J. Y. C. Chen and M. J. Barnes, "Human–agent teaming for multirobot control: A review of human factors issues," *IEEE Trans. Human-Mach. Syst.*, vol. 44, no. 1, pp. 13–29, Feb. 2014.
[40] ROBOTIS e-Manual. (2021). *Overview*. Accessed: Aug. 2021. [Online]. Available: http://emanual.robotis.com/docs/en/platform/turtlebot3/overview/
[41] e-con Systems. (2021). *See3CAM_130—Documents*. Accessed: Aug. 2021. [Online]. Available: https://www.e-consystems.com/doc_13MP_autofocus_USB3_Camera.asp
[42] S. Wang, Y. Liu, Y. Qiu, Q. Zhang, F. Huo, Y. Huangfu, C. Yang, and J. Zhou, "Cooperative task allocation for multi-robot systems based on multi-objective ant colony system," *IEEE Access*, vol. 10, pp. 56375–56387, 2022.
[43] Y. Wu, T. Liang, J. Gou, C. Tao, and H. Wang, "Heterogeneous mission planning for multiple UAV formations via metaheuristic algorithms," *IEEE Trans. Aerosp. Electron. Syst.*, vol. 59, no. 4, pp. 3924–3940, Aug. 2023, doi: 10.1109/TAES.2023.3234455.

OMAR AL-BURAIKI (Member, IEEE) received the Ph.D. degree in electrical and computer engineering from the School of Electrical Engineering and Computer Science, University of Ottawa, Ottawa, ON, Canada. He is currently a Postdoctoral Fellow with the Department of Mechanical and Mechatronics Engineering, University of Waterloo. His research interests include machine intelligence, robotics, automatic control, autonomous systems, and AI/ML-based robotic vision.

PIERRE PAYEUR (Member, IEEE) received the Ph.D. degree in electrical engineering from Université Laval, Canada. Since 1998, he has been a Professor with the School of Electrical Engineering and Computer Science, University of Ottawa, Canada. He is currently the Director of the Sensing and Machine Vision for Automation and Robotic Intelligence Research Laboratory. He is a Founding Member with the Vision, Imaging, Video, and Autonomous Systems Research Laboratory. His research interests include machine vision, tactile sensing, automation, robotics, and computational intelligence.